

Imbibition, desiccation and mechanical deformations of zein pills in relation to their porosity

M.A. Sabino¹, L. Pauchard^{2,a}, C. Allain², P. Colonna¹, and D. Lourdin¹

¹ Institut National de la Recherche Agronomique (INRA), Unité de Recherche sur les Polysaccharides leurs Organisations et Interactions (URPOI), BP 71627, 44316 Nantes Cedex 03, France

² Laboratoire FAST (Fluides, Automatique et Systèmes Thermiques), UMR 7608, Bât. 502, 91405 Orsay Cedex, France

Received 14 October 2004 and Received in final form 2 December 2005 /

Published online: 11 May 2006 – © EDP Sciences / Società Italiana di Fisica / Springer-Verlag 2006

Abstract. This paper deals with the interaction between zein (the main protein component of corn grain) and water. It induces macroscopic properties changes and may allow for the understanding of the basis of zein endosperm structure: vitreous endosperm is compact and floury endosperm is porous, giving the endosperm its hard and soft textures, respectively. In that aim porous pills made by compaction of zein powder submitted to different hydration/dehydration processes have been prepared and studied. In particular, imbibition measurements of a pure-water drop deposited onto a zein pill were performed. Also, desiccation of a zein pill previously imbibed induces strong mechanical stresses leading to crack formation and/or large deformations.

PACS. 61.43.Gt Powders, porous materials – 87.15.La Mechanical properties – 46.32.+x Static buckling and instability

A deeper understanding of the structural and mechanical properties of cereal grains in relation to genetics, on the one hand, and to differences in temperature and hygrometry linked to climatic variations, on the other, is a major issue for agronomy and the food industry today [1–4]. The endosperm of corn grains is the part which is mainly composed of semi-crystalline starch granules (approximately 85% in weight) of about 30 μm in size and of a protein (approximately 10% in weight) filling interstitial spaces. It is the noble part of cereal grains which is fractionated to obtain the flour. Despite numerous studies focused on ultra structure and histochemistry, however, there is a lack of understanding of the mechanisms linked to desiccation and preceding the floury and vitreous domains formation, constituting the endosperm of grains. The corn protein is mainly composed of zein (45–50% on a dry basis), which is hydrophobic and soluble in aqueous ethanol (70%) [2–4].

Despite its hydrophobicity, the interaction of zein with water under humidity rate variations plays a key role. Indeed, during zein dehydration, for a given water content which depends on the temperature, the protein becomes glassy and thus its mechanical properties dramatically change [5]. So, although the protein concentration in the corn endosperm is low, it seems that zein plays an important role on the final texture of mature grain.

In order to study how the interaction between zein and water-induced macroscopic properties changes, we have used pills made by compaction of fine zein powder. Different experiments have been performed: first we have studied the macroscopic aspect and the microstructure of pills that have been submitted to different hydration/dehydration processes. Second the imbibition and wetting properties have been measured and the results have been related to water/zein interaction. Finally, due to the volume variations and to glass transition induced by dehydration, large stresses appear that may lead to the formation of cracks or to the buckling of the material.

The paper is organised as follows: the materials and the methods are described in Section 1. The evolution of pills under different water hydration/dehydration processes is studied in Section 2. Imbibition of a drop into a porous pill is investigated in Section 3. Finally mechanical instabilities, *i.e.* deformation and/or cracks formation, which occur during imbibition and the desiccation process of the saturated porous pill, are described in Section 4.

1 Experimental methods

1.1 Materials and pill preparation

The used zein protein was obtained from Fluka Biochemika (Germany). Fractions of protein had a molecular

^a e-mail: pauchard@fast.u-psud.fr

weight between 25 and 29 kDa (determined by EDS electrophoresis). The protein water content was 5.3% determined by TGA and verified by Karl Fischer method.

The pills of 16 mm diameter were made from different weights of zein powder, depending on the thickness expected (250 mg for 1 mm thickness), and were moulded in a hydraulic press by one compression cycle: a) 15 s at 100 kg/cm², b) 15 s at 0 kg/cm² and c) 30 s at 120 kg/cm². In the following the pills used without any treatment after their preparation (*i.e.* hydration/dehydration) are denoted as initial pills.

1.2 Sample hydration/dehydration of zein pills

Different hydration/dehydration conditions were used: two different temperatures $T = 25\text{ }^{\circ}\text{C}$ and $40\text{ }^{\circ}\text{C}$ and three different paths were considered:

- a) The pills were put on a glass support and —with a micropipette— 100% of distilled water (which corresponds to 50% based on the total weight of each hydrated pill) was added. After that, they were introduced into an isolated vapour system in the presence of P₂O₅ powder, and they were left under these conditions for approximately one week (when their weight was stabilized).
- b) Pills were humidified as previously by adding 100% (dry matter) distilled water (which corresponds to 50% based on the total weight of each hydrated pill) and afterwards they were then introduced into an atmosphere where relative humidity was controlled by saturated salt solutions in order to be dehydrated. The drying process began with BaCl₂ (90% relative humidity at 25 °C) until the pill weight was constant (several days were necessary to reach equilibrium for each salt). This process was subsequently repeated for the other salts: NaCl (75%), NaBr, (57%) K₂CO₃ (43%), MgCl₂ (33%) and CaCl₂ (29%) (with their corresponding relative humidity at 25 °C). This dehydration process took approximately 21 days.
- c) The pills were introduced into an isolated vapour system with saturated water vapour (*i.e.* 100% relative humidity) at room temperature, until the pills reached a constant weight (which was approximately 35% of water content, based on the total weight of each sample) and afterwards the pill were dried using the “slow-drying” process as in b).

1.3 Physicochemical methods of characterization

Scanning electron microscopy

With the purpose of seeing the internal morphology of the pills, samples were fractured after immersing them in liquid nitrogen. The samples were gold/platinum coated in a Polaron SC502 Sputter coater (FISON) and a Scanning Electron Microscope Stereoscan 440 (OXFORD) was employed for the observations of the surfaces and morphology of samples. Low voltages were used to guarantee minimum radiation damage to the samples.

Water analysis in dehydrated pills

Water concentration was determined by thermogravimetric analysis (TGA 2050, TA Instruments, USA) under a nitrogen atmosphere and was properly gauged, the heating scan ranged from 25 °C up to 130 °C. Samples were left at 130 °C for 45 minutes until total weight balance.

Glass transition temperature determination

The determination of the glass transition temperature (T_g) for various water contents was performed using thermal analysis with a DSC-121 equipment (SETARAM, France) (see Ref. [5]).

1.4 Imbibition measurements

Imbibition of drops was investigated onto zein pills in order to measure the porosity and the pore size of the pills. Just after its deposition the drop is monitored by simultaneously side and top views using CCD cameras. Then the acquired images were analyzed by an image processing software (Image Pro Plus). This allows for the determination of the drop characteristics during its imbibition: contact angle of the drop with the pill, basal radius, apex height and infiltrated zone radius. In the case of slow imbibition, some experiments were performed to measure the time variations of the mass of the pill after deposition of the drop. In our experiments, a pill is deposited on a balance and the drop is monitored in top view.

2 Evolution under different hydration/dehydration histories

Figure 1 displays pictures taken at the end of the dehydration process for the different protocols used (see Sect. 1.2). For dehydration at 40 °C the samples always exhibit a brown coloration and a smooth and shiny surface. On the contrary, those dehydrated at 25 °C all present a yellowish coloration and a slightly rough superficial aspect. In both cases the pills had become more rigid than the initial moulded zein pills. It is also apparent in Figure 1 that all the samples humidified by adding water (using protocols a) or b)) undergo a deformation: the pills do not remain flat. This deformation is larger when dehydration is rapid (in the presence of P₂O₅ —protocol a)). In the same figure, we have also reported for each case the water content ω_w and the temperature of glass transition, T_g , measured at the end of dehydration. A good agreement is found between these measured values and the data reported in the literature [5, 6]: for increasing water content, the glass transition temperature rapidly decreases (graph in Fig. 1). Also our measurements appear to be dispersed in comparison with the data from references [5, 6]. This suggests a correlation between experimental results and the protocol used for zein hydration. On the contrary, for a given

salts	Protocol (a) fast hydr. / fast dehydr.		Protocol (b) fast hydr. / slow dehydr.		Protocol (c) slow hydr. / slow dehydr.	
	T=40°C	T=25°C	T=40°C	T=25°C	T=40°C	T=25°C
P₂O₅ fast dehydration						
BaCl₂ → CaCl₂ slow dehydration						
T_g (°C)	115	110	64	62	68	63
ω_w (%)	3.1	3.3	4.6	4.8	4.8	5.5

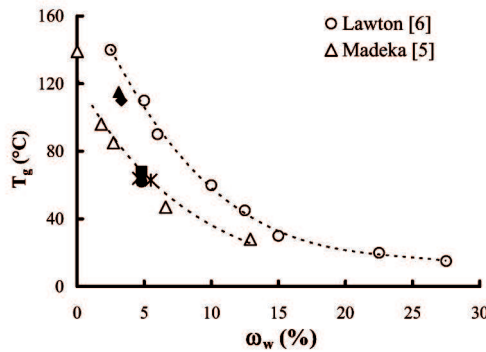


Fig. 1. Table: appearance of the zein pills after dehydration under different conditions and temperatures. The values of the vitreous transition (T_g) and the final water content in the samples (ω_w , % total) are included. Thickness is the same for each pill. Graph: T_g vs. water content of zein samples subjected to different protocols hydration/dehydration: experimental measurements from the table correspond to dark symbols and (\circ , Δ) correspond to literature data (lines are only to guide eyes).

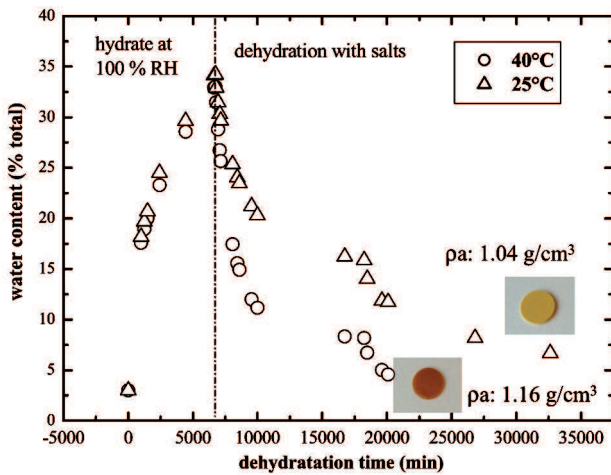


Fig. 2. Variation of the water content (% total) in the moisturized samples (100% RH) and later dehydrated in the salts at two different temperatures: 25 °C and 40 °C. The empty symbols are the same as in Figure 1, the final appearance of the dehydrated pills is shown for each temperature.

temperature, T , there exists a range of water contents, $\Delta\omega_{wg}(T)$, such that at water content $\omega_w > \Delta\omega_{wg}(T)$ the medium is rubbery while at water content $\omega_w < \Delta\omega_{wg}(T)$ it is glassy, where $\Delta\omega_{wg}(T)$ is a decreasing function of T .

If a water drop is deposited on these pills we observe that it nearly never infiltrates except in the case of a slow dehydration at 25° after a humidification in a vapour sat-

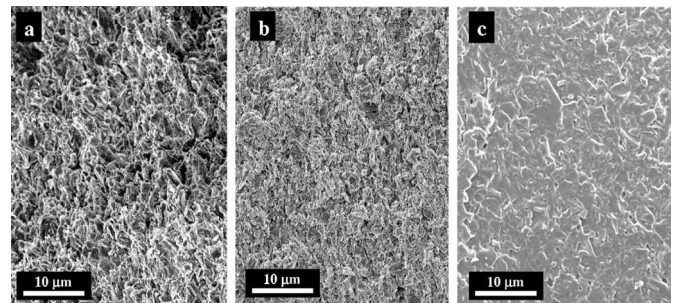


Fig. 3. SEM microphotographs of the inner structure of thin zein pills: (a) initial zein pill; (b) and (c) zein pills dried at 25 °C and 40 °C in presence of salts according to protocol b), respectively.

urated in water (protocol c)). In order to understand these results, let us consider first the case of protocol c). Figure 2 presents the sorption/desorption kinetics at the two different temperatures used. While in both temperatures the dehydration is slow, the final appearance is clearly different, as has been previously mentioned. For each sample, the apparent density has been measured at the end of the dehydration: it was found that the sample dehydrated at 25 °C (1.04 g/cm³) has a smaller density than those dehydrated at 40 °C (1.16 g/cm³). SEM microphotographs had also been done to observe the inner structures of initial zein pills and zein pills prepared following different protocols (see Fig. 3). The initial zein pills show a dense

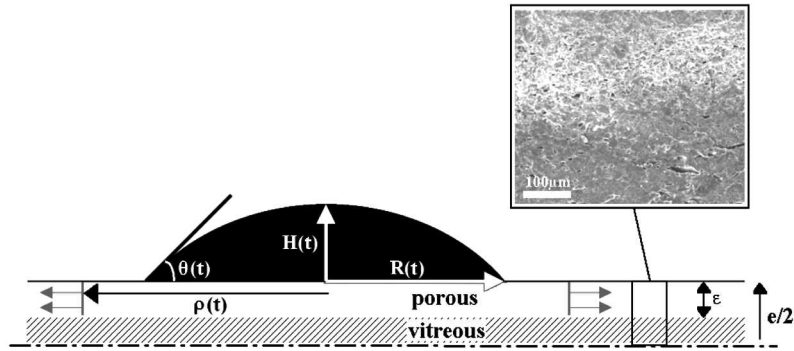


Fig. 4. Cross-section of an imbibing drop over a porous zein pill. The flow of liquid in the porous network is mainly radial and takes place only in the upper porous layer that is limited by the vitreous compact region. Note that the portion of vitreous compact region in the thickness of the pill is exaggerated for a better observation.

porous structure (Fig. 3a). For a dehydration temperature equal to 25 °C (protocol b)) the core of the pill is more compact (Fig. 3b) while for dehydration at 40 °C (protocol c)) (Fig. 3c), except for some voids, a compact state is observed on almost all the depth of the pill.

To return to the cases where humidification is done by adding liquid water (protocols a) and b)), SEM microphotographs have shown that, for a dehydration temperature $T = 25$ °C, the structure is compact in the core and porous on the pill surface as shown in the cross-section in Figure 4 (thickness is of the porous layer $\cong 200$ μm). This porous layer is responsible for the low density and imbibition capacity. It also explains the yellowish coloration and a slightly rough superficial aspect. It has been demonstrated in a previous work [5] that these differences in structure and properties are due to the kinetics of dehydration in relation to the glass transition of zein in the presence of water. Since the water content in the core of the pill decreases more slowly during dehydration, an evolution of the structure leading to compaction has time to take place in that region.

So we observe that different hydration/dehydration histories lead to differences in the pill macroscopic and microscopic structure. The coloration and surface aspect is not representative of the infiltration capacity and of the microstructure of the pill which can be mainly compact while its surface remains porous or solely rough. In all the cases the glass transition, *i.e.* $\omega_{\text{wg}}(T)$, is found, as expected, independent of the dehydration kinetics and the observed values are in agreement with the literature results. The slow dehydration of pills that have been humidified in a vapour saturated of water (protocol c)), allows, by changing the temperature, to obtain glassy zein either in a compact or in a porous state.

3 Imbibition measurements

A porous medium is characterized by its porosity and by the pore size. The porosity is defined as the ratio of the pore volume divided by the total volume of the medium. These two quantities can be measured by studying the spontaneous penetration of a pure-water drop into the

medium [7]. Since the zein pills are made by compaction of zein powder, the pores are assumed to be connected to each other. The time evolution of drops deposited on zein pills was studied for pills prepared following protocols b) and c) (see Sect. 1.2). Just after its deposition, the time variations of the geometrical characteristics of the drop were measured: the basal radius, R , the apex height, H , and the contact angle on the pill surface, θ ; also, the radius of the infiltrated wetted region, ρ , was measured (see sketch in Fig. 4). The results obtained for the contact angle are shown in Figure 5 for each case. Whatever the pill studied, while the values of θ and H decrease with time, the basal radius remains stationary due to the roughness of the pill surface responsible for the pinning of the drop edge [8]. During the first 25 seconds, the contact angle of the drop deposited on the pills dehydrated at 25 °C decreases more rapidly than for the pills dehydrated at 40 °C.

The variations of the drop volume with time were also deduced from the measurements of the contact angle and the apex height, assuming the axisymmetry of the drop (Fig. 5b). We can easily verify that the drop keeps a spherical cap shape all along the imbibition process. In the case of the pill dehydrated at 25 °C, protocol b)), the drop volume rapidly decreases with time and the drop is almost completely infiltrated after 25 s. For the other pills, the drop volumes vary only slowly with time suggesting a very slow imbibition of the drops. In the case of the pill prepared according to protocol c)), the imbibition process is followed by a swelling which occurs all around the drop edge.

The porosity of the infiltrated layer can be deduced from the knowledge of the drop volume, V_{drop} , and the radius of the infiltrated region, ρ . Assuming that the main process in the liquid imbibition into the porous medium set in a radial flow inside the upper porous layer of the pill which has a thickness ε , the drop volume expresses as

$$V_{\text{drop}}(t) = V_0 - V_{\text{swelling}}(t) - V_{\text{liq}}(t) \quad \text{and} \\ V_{\text{liq}}(t) = K\pi\varepsilon\rho^2(t), \quad (1)$$

where V_0 is the initial drop volume, V_{swelling} is the volume of the swelling part of the pill during the imbibition

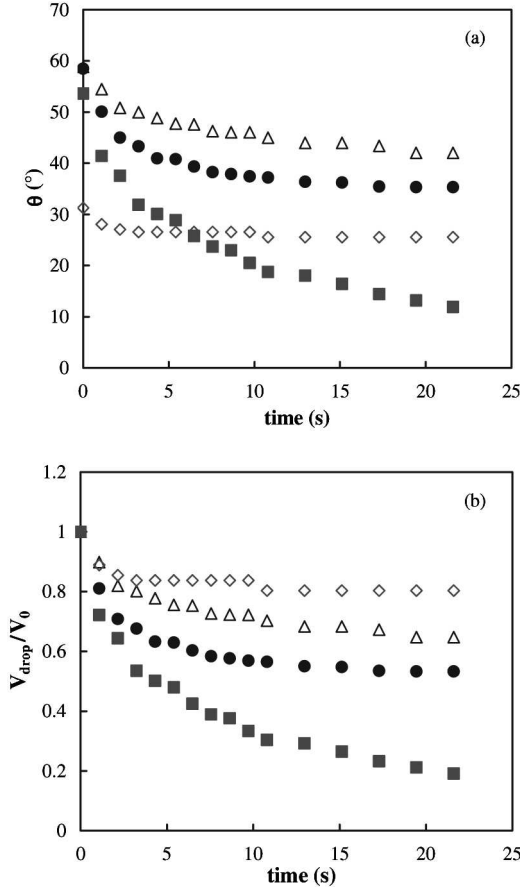


Fig. 5. Time variations of the contact angle (a) and time variations of normalized volume of drops deposited on zein pills (b) prepared following different protocols. Pill introduced in a saturated water vapour system then dehydrated at 25 °C (●) according to protocol c) ($V_0 = 19 \text{ mm}^3$); pill introduced in a saturated water vapour system then dehydrated at 40 °C (△) according to protocol c) ($V_0 = 17 \text{ mm}^3$); pill dehydrated at 25 °C (■) according to protocol b) ($V_0 = 29 \text{ mm}^3$); pill dehydrated at 40 °C (◇) according to protocol b) ($V_0 = 11 \text{ mm}^3$).

process (estimated by side view visualisation), V_{liq} is the volume of liquid inside the porous layer of the pill and K its porosity. So the side and top views are required to measure $V_{\text{drop}}(t)$, $V_{\text{swelling}}(t)$ and $V_{\text{liq}}(t)$, respectively. Direct observation in top view allows us to obtain the radius of the infiltrated region, ρ , as a function of time as described in Figure 6. Measurements of $V_{\text{drop}}(t)$ correlated to ρ can be fitted by expression (1). For the pill dehydrated at 25 °C (protocol c) the porosity is found to be: $K = 0.45 \pm 0.02$.

In the following let us evaluate the pore size of the same pills. The liquid contained within the porous layer spreads under the influence of capillary forces. The kinetics two-dimensional circular spreading was first studied by Gillespie [9,10]. The radius of the wetted region, $\rho(t)$ expresses as

$$\rho^2(t)(\rho^4(t) - \rho_0^4) = \frac{3b\kappa\gamma \cos(\theta^*)}{2c_s^3\eta} \left(\frac{3V_0}{2\pi\varepsilon}\right)^2 t, \quad (2)$$

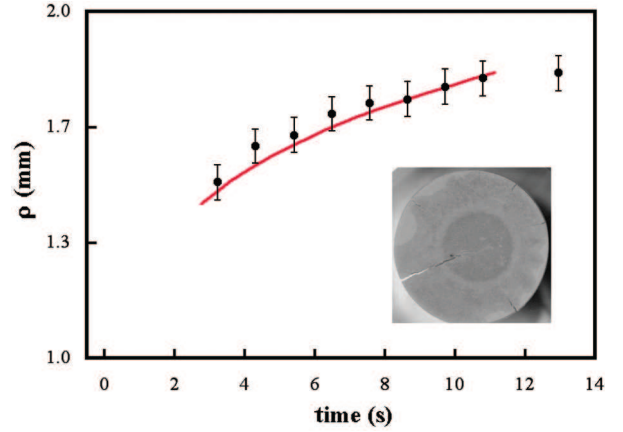


Fig. 6. Time variations of the radius of the wetted region measured by top view. The line corresponds to the theory. Inset: digitized image of a zein pill dried at 25 °C in presence of salts. Radial cracks forms at the end of the infiltration of the drop.

where ρ_0 is the radius of the infiltrated region at time zero which scales with the pore size, b denotes a constant descriptive of the substrate and c_s the saturation concentration of the liquid in the substrate in accordance with [11], γ the surface tension water/air, θ^* is the advancing contact angle ($\cong 60^\circ$ here), η the viscosity of the liquid, $\varepsilon \approx 200 \mu\text{m}$ (see Fig. 4) denotes the thickness over which the radial flow takes place and the parameter κ is the permeability which is proportional to the square of the pore size according to the Kozeny-Carman law [12]:

$$\kappa = \frac{1}{180} \frac{K^3}{(1-K)^2} (2r_{\text{pore}})^2. \quad (3)$$

Fitting the experimental measurements by expression (2) allows for an evaluation of the permeability: $\kappa = 10^{-15} \text{ m}^2$ and thus of the pore size $2r_{\text{pore}} = 0.5 \mu\text{m}$ for pills dehydrated at 25 °C, protocol b). This estimation is in agreement with the measurements in the SEM in Figure 3b. Indeed, statistics by direct observation of the SEM microphotograph in Figure 3b give the mean radius of pore size equal to $0.3 \mu\text{m}$ with an inaccuracy of 50%.

In our experimental situations, *i.e.* imbibition of a drop of about 10 mm^3 , the characteristic time of imbibition denoted by $t_{\text{imbibition}}$ does not exceed 25 s. We can compare this value to two other time scales. Firstly, the characteristic drying time, t_D , of a sessile drop having a volume V_0 , a surface S_0 and a basal radius R_0 , at $t = 0$. It can be defined by [13]

$$t_D = (V_0/(R_0S_0)) \times (R_0/V_E) \quad (4)$$

taking into account that the geometrical factor $V_0/(R_0S_0)$ strongly increases with θ_0 ; V_E is the mean water flux per unit surface computed from profile recording of a sessile drop; in our experimental situations V_E is about 10^{-4} mm/s . Thus, the order of magnitude of t_D is 5000 s much larger than the time needed for the drop to disappear from the pill surface. So, evaporation has a negligible effect on the imbibition process in this experiment.

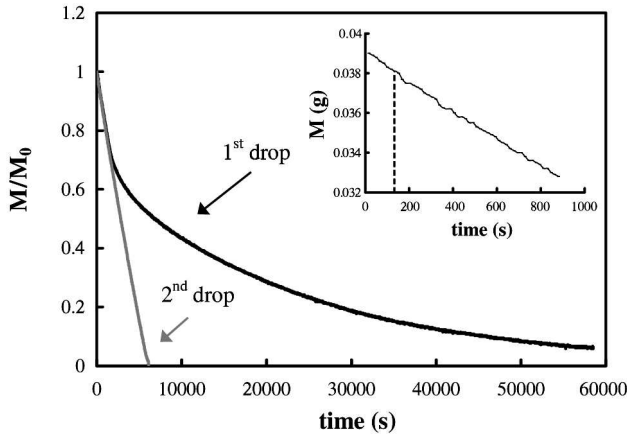


Fig. 7. Variation of the normalized water mass (M/M_0) as a function of time for zein dehydrated slowly at 25 °C, according to protocol b). Two experiments are reported. In the first, a drop is deposited on a dry pill (mass of the first drop $M_0 = 39 \cdot 10^{-3}$ g); it completely infiltrates and dries (black line). In the second experiment, after deposition of a first drop a second one ($M_0 = 30 \cdot 10^{-3}$ g) is deposited 10 min later on the basal region previously wetted and dries as a drop deposited on a non-porous substrate (grey line). Inset: mass variation *vs.* time for the first drop: the dashed line marks the end of imbibition of water. The mass of the dry pill is $250 \cdot 10^{-3}$ g.

Secondly, it is interesting to consider the time for imbibition in the vertical direction. In accordance with the Darcy law, this time scales as [14]

$$t_e \cong \frac{\varepsilon^2 \eta}{\kappa p_c}, \quad (5)$$

where p_c denotes the capillary pressure driving the imbibition process ($p_c \cong 2 \cdot 10^6$ Pa). Finally t_e is estimated as 1 s. This allows for a confirmation that in the case of the drop into a thin zein pill, radial imbibition is the main process.

Once the drop is completely infiltrated in the pill, the liquid evaporates from the exposed surface of the porous network. During the drying process, the time variation of the mass of water was measured and results are shown by the black line in Figure 7. After the constant rate period in which water evaporates from the surface of the pill in the air and is replenished by flow from the interior of the network, the time variation of the mass slows down. Usually this second stage is characterized by an internal moisture migration which limits the replenishment of water towards the surface of evaporation. In our case since the zein protein interacts with water, the porous structure also evolves. Indeed, the aspect of the region of the pill which has been wetted is different from the unwetted region, as has been noted in Section 2. To investigate this point after deposition of a first drop, a second drop is deposited on the previously wetted surface of the pill; the second drop has a contact base lower than the first one to recover only the part already saturated. In this case a very low imbibition takes place and the contact angle of the second drop is large, of the order of 75°. The region previously wetted has become less porous, the interaction

of water with zein leads to the filling of a part of the pores. Figure 7 shows the dimensionless water mass variations *vs.* time for the second drop when two drops are successively deposited on the same pill. Practically the second drop dries as a drop deposited on a non-porous substrate, *i.e.* the time variation of the mass is linear as expected when the evaporation is limited by diffusion of water in the air. Results are the same even if the time elapsed between the depositions of both drops is 10 minutes or one hour.

4 Mechanical instabilities

The mechanical properties of the zein pills are strongly dependent on their preparation, in particular on the dehydration rate. Initial zein pills are very brittle, which is related to a low cohesion strength due to a simple adhesion through contact between grains. Hence, during the imbibition of a water drop on such pills, cracks occur very rapidly after the drop deposition and then large deformations take place. In the case of a zein pill dehydrated at 40 °C, according to protocol a), a stronger cohesion strength takes place between grains: the rigidity is much more important. An intermediate cohesion strength exists for zein pills dehydrated at 25 °C, according to protocol b): a partial coalescence takes place between grains leading to a medium both more rigid than the initial one and more porous than the pills dehydrated at 40 °C. In the following we only consider initial zein pills.

A porous network undergoes large mechanical stresses during both imbibition of a drop and desiccation after saturation. Since the two primary modes of deformation which are liable to occur are in-plane stretching and out-of-plane bending, the mechanical stresses can be relaxed by inducing different deformations and/or cracking as described by the images of final shapes in Figures 8a and b. In this way inhomogeneous hydration was investigated by depositing drops of different size at the center of the surface of several pills.

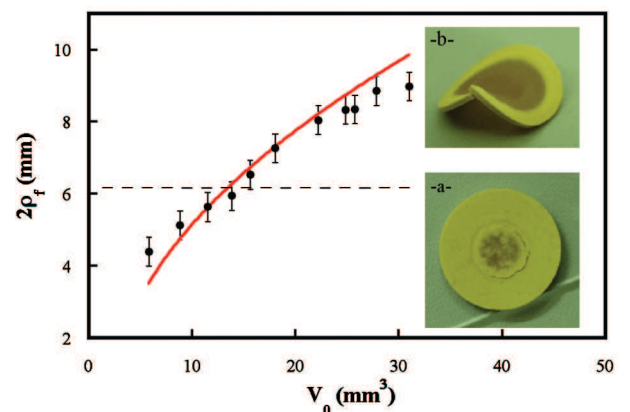


Fig. 8. Maximum value of the diameter, $2 \times \rho_f$, of the wetted region *vs.* volume, V_0 , of the deposited drop. Photographies of zein pills on which a drop of increasing initial volume has been deposited (pill dimensions: 16 mm in diameter and 1 mm thick): (a): $V_0 = 28 \text{ mm}^3$; (b): $V_0 = 6 \text{ mm}^3$.

Two time scales can be distinguished. In the short time scale, the imbibition of the liquid into the porous pill takes place as described in Section 3. The time variations of the drop volume changes are given by (1). As soon as the drop disappears from the surface of the pill, the maximum value of the radius, ρ_f , of the wetted region, *i.e.* the saturated region, can be estimated as a function of the initial drop volume for a given porous pill:

$$\rho_f = \left(\frac{V_0}{\pi K e} \right)^{1/2}. \quad (6)$$

By fitting this law with measurements of the radius of the wetted region, ρ_f , as a function of the initial drop volume, V_0 , the porosity of the initial zein pill can be estimated (Fig. 8). We found $K = 0.63 \pm 0.02$. This value is greater than the porosity measured for pills dehydrated at 25 °C, RH = 100%. Such large porosity is characteristic of an ensemble of small grains, displaying a non-spherical shape and strong friction effects. Also, during the imbibition of the drop the wetted central region of the pill is submitted to an extension as described in Figure 9—sketch (a). In this case two behaviours can be distinguished depending on the relative values of ρ_f and the radius of the whole pill, ρ_2 . If ρ_f is just smaller than ρ_2 (thin unsaturated ring), radial cracks preferably propagate at short time scale, that is before the drop has completely infiltrated the pill or just after (see image in Fig. 8b). Radial cracks are induced by the orthoradial component, $\sigma_{\theta\theta}$, of the mechanical stress field in the ring (see inset (a) in Fig. 9). Otherwise if the wetted region has a radius ρ_f small compared to the pill radius, ρ_2 , (wide ring) the orthoradial component is lower than in the previous case and no crack forms in the short time scale.

At longer time scale, the saturated part of the pill is equivalent to a porous material with pores filled of solvent which dries. As a consequence, the pressure in the liquid is not uniform [15]: the tension in the liquid is greater near the drying surface leading to consequently greater contraction of the network there. Capillary tension generates important stresses resulting in some deformations of the network. The capillary pressure is estimated as

$$p_c = \frac{-2\gamma \cos(\theta^*)}{r_{\text{pore}}} \cong 2 \cdot 10^6 \text{ Pa}. \quad (7)$$

Here the negative sign indicates that the liquid is in tension. During the drying process of the saturated pill, the wetted central part is in compression due to the shrinkage of the network (sketch (b) in Fig. 9). Also when ρ_f is much smaller than ρ_2 (wide unsaturated ring), the wetted central region becomes under compression due to drying at long time scale. Thus, a circular crack forms (image in Fig. 8a).

Otherwise the observation of a saturated pill during water evaporation shows that the pill does not remain plane: deformations can take place both at short and long time scales. Here, the deformations are not due to a swelling of the pill as described in Section 3 but they are out-of-plane displacements of the pill surface leading

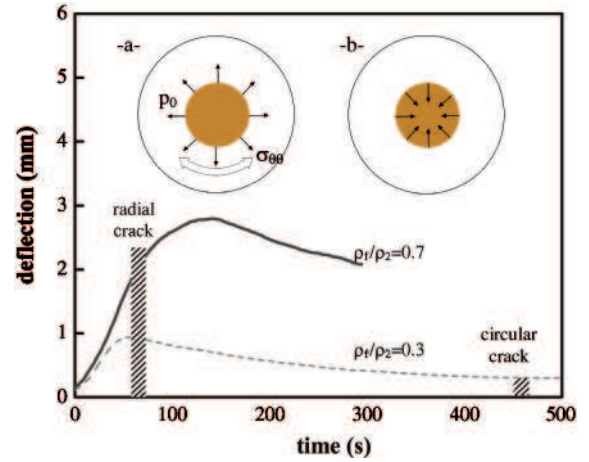


Fig. 9. Time variations of the surface displacement measured at the border of the pill diameter from the periphery. The displacement is measured in both cases: for a pill displaying a large wetted region ($\rho_f/\rho_2 = 0.7$, black line) and another displaying a small one ($\rho_f/\rho_2 = 0.3$, dashed grey line). The thick vertical dashed lines indicate the formation of crack; the thickness of the lines is related to the inaccuracy for the determination of the fracture nucleation time. The schematic illustration of the orthoradial component of the stress field, $\sigma_{\theta\theta}$, in an unsaturated ring surrounding a region submitted to an extension, $p_0 > 0$ in (a). In sketch (b) the wetted central region is submitted to a compression, $p_0 < 0$. Imbibition time/dehydration time are, respectively, 50 s/30000 s in the case of a small wetted region and 90 s/50000 s in the case of a large wetted crack.

to bending the pill. Also it is noticeable that the larger is the size of the wetted central part, the larger is the deformation of the pill. Such deformations were studied during both imbibition and desiccation processes of the saturated part for two ratios ρ_f/ρ_2 (see Fig. 9). The deflection, *i.e.* the out-of-plane displacement of the pill surface, was investigated using video recordings and image analysis. For ρ_f/ρ_2 close to 1 large bending occurs leading usually to horse-saddle shape at the final stage of the desiccation process. Such shapes are characteristic of the minimal surface where deformation is principally due to bending. On the other hand, when ρ_f/ρ_2 is smaller than 1, deflection is lower. In this case the circular crack which forms at long time scale relaxes a great part of the residual stresses in the porous network leading in the following to only low out-of-plane deformations (Fig. 9).

5 Conclusion

The interaction between zein which is one of the main components of the corn protein and water has been studied. In this purpose different pills were made by compaction of fine zein powder according to several protocols (hydration/dehydration processes). Imbibition processes of a pure-water drop deposited on such a given pill have been performed and revealed a swelling of the saturated part of the pill. Also, dynamics of the imbibition process allows for an evaluation of the pore size of the saturated

part of the pill. Moreover, it was shown that the mechanical properties of the zein pills are clearly dependent on their preparation. In the case of initial zein pills, these last exhibit brittleness properties and mechanical instabilities occur leading to cracks formation and strong deformations (horse-saddle shape).

References

1. R.V. Kowles, R.L. Phillips, *Int. Rev. Cytol.* **112**, 97 (1988).
2. O. Olsen, R. Potter, R. Kalla, *Seed Sci. Res.* **2**, 1 (1992).
3. M.A. Lopes, B.A. Larkins, *Plant Cell* **5**, 1383 (1993).
4. A.M. Clore, J.M. Dannenhoffer, B.A. Larkins, *Plant Cell* **8**, 2003 (1996).
5. H. Madeka, J.L. Kokini, *Cereal Chem.* **73**, 433 (1996).
6. J.W. Lawton, *Cereal Chem.* **69**, 351 (1992).
7. M. Alava, M. Dubé, M. Rost, *Adv. Phys.* **53**, 83 (2004).
8. L. Bacri, F. Brochard, *Eur. Phys. J. E* **3**, 87 (2000).
9. T.J. Gillespie, *Colloid. Sci.* **13**, 32 (1958).
10. E. Kissa, *J. Colloid Interface Sci.* **83**, 265 (1981).
11. A. Bohran, K.K. Rungta, *J. Colloid Interface Sci.* **158**, 403 (1993).
12. F.A.L. Dullien, *Porous Media: Fluid Transport and Pore Structure* (Academic Press, San Diego, 1979).
13. L. Pauchard, C. Allain, *Phys. Rev. E* **68**, 052801 (2003).
14. V.M. Starov, S.R. Kostvintsev, V.D. Sobolev, M.G. Velarde, S.A. Zhdanov, *J. Colloid Interface Sci.* **252**, 397 (2002).
15. C.J. Brinker, G.W. Scherer, *Sol-gel Science* (Academic Press Inc., 1990).